An efficient and novel numerical method for quasiconformal mappings of doubly connected domains

Prabir Daripa and Daoud Mashat
Department of Mathematics, Texas A&M University, College Station, TX 77843-3368, USA

Received 10 November 1997; revised 28 May 1998
Communicated by M.H. Gutknecht

A numerical method for quasiconformal mapping of doubly connected domains onto annuli is presented. The ratio R of the radii of the annulus is not known a priori and is determined as part of the solution procedure. The numerical method presented in this paper requires solving iteratively a sequence of inhomogeneous Beltrami equations, each for a different R. R is updated using a procedure based on the bisection method. The new method is an extension of Daripa's method for the quasiconformal mapping of the exterior of simply connected domains onto the interior of unit disks [15]. It uses fast and accurate algorithms for evaluating certain singular integrals and is, thus, very efficient and accurate. Its performance is demonstrated for several doubly connected domains.

Keywords: quasiconformal mapping, Beltrami equation, fast algorithm

AMS subject classification: 17-08, 30C75, 45G05, 65E05, 65Y20

1. Introduction

The theory of quasiconformal mappings is nearly 70 years old and seems to have been started by Ahlfors [1], Grötzch [18], Lavrentjev [19] and Morrey [23]. Grötzsch [18] defines quasiconformal mappings, which can be viewed as a generalization of conformal mappings, as mappings whose linearizations transform circles into ellipses for which the quotient of the lengths of the axes is bounded, while Lavrentjev [19] constructs such mappings satisfying elliptic systems of partial differential equations. All the standard definitions of quasiconformal mappings [20] are, in general, based on direct generalizations of certain characteristic properties of conformal mappings, and several fundamental theorems on analytic functions remain valid for quasiconformal mapping, at least in a modified form (cf. [20]). A systematic introduction into the theory of quasiconformal mapping can be found, for instance, in Lehto and Virtanen [20].

Quasiconformal mappings have been studied extensively in complex analysis (cf. [1,2,19,20]). Interest in them is partly for its own sake and partly due to their applications to differential equations, complex analysis, topology, Riemann mappings, complex dynamics and grid generation. A concise description of some of these applications can be found in review articles by Bers [6] and Carleson and Gamelin [10]. Applications to numerical grid generation can be found in Belinskii et al. [3], Daripa [13] and Mastin and Thompson [21]. Applications to subsonic flow problems, quasilinear second-order partial differential equations, and systems of first order equations in the plane can be found in Bers [5,7,8]. Even though significant progress in the theory of quasiconformal mappings and its application towards proving important results in applied as well as pure fields has been made, progress on numerical methods has been very slow. In fact, numerical quasiconformal mapping techniques are of much more recent origin. This is partly due to difficulties in finding convergent iterations for such mappings.

There has been some recent work on numerical quasiconformal mapping techniques based on solving elliptic equations in the real plane with finite difference or finite element methods. For example, Belinskii et al. [3] and Mastin and Thompson [21] use finite difference methods. Some of these methods are difficult to implement for arbitrary regions. A finite difference scheme for constructing quasiconformal mappings for arbitrary simply and doubly-connected region of the plane onto a rectangle was developed by Mastin and Thompson [22]. Vlasynk [30] also considers such a scheme for mappings of doubly connected and triply connected domains onto a parametric rectangle. A finite element based method was developed by Weisel [31].

Very little work has been done on the numerical construction of quasiconformal mappings in the plane using the Beltrami equation (2.3) defined in section 2. A probable reason for this is the lack of efficient and accurate techniques for evaluating singular integral operators that arise in solving this equation. Another reason for the lack of suitable quasiconformal mapping algorithms is that such algorithms are inherently iterative and nonlinear in nature and must be convergent for a suitable set of examples. In [14] Daripa presented a fast algorithm for the accurate evaluation of one of the singular operators that arise in this context. It was subsequently used by Daripa [15] for numerical quasiconformal mappings of exterior of simply connected domains onto the interior of a unit disk using the Beltrami equation. Daripa [15] was the first to use the Beltrami equation to propose an efficient numerical quasiconformal mapping technique which is also convergent based on numerical evidence. This method is extended here to the quasiconformal mapping of an arbitrary doubly connected domain with smooth boundaries onto an annulus $\Omega_R = \{\sigma\colon\ R < |\sigma| < 1\}$. One of the added difficulties here over similar techniques for simply connected domains is that R is not known a priori.

This paper is laid out as follows. In section 2 we present some mathematical preliminaries required for the construction of quasiconformal mapping algorithms within an annulus. In section 3, we formulate a boundary value problem for quasiconformal mappings of doubly connected domains. In section 4, we present the numerical method for quasiconformal mappings of doubly connected domains onto annuli. In section 5, we discuss some numerical results.

2. Mathematical preliminaries

In this section we present the mathematical background on quasiconformal mappings of doubly connected domains onto annuli. Quasiconformal mapping which satisfies a nonlinear partial differential equation of the type

$$z_{\bar{\sigma}} = f(\sigma, z, z_\sigma) \tag{2.1}$$

has been investigated by Bojarski and Iwaniec [9]. Here, $z(\sigma)$ is a complex valued function of complex variables σ and $\bar{\sigma}$, and $\partial/\partial\sigma$ and $\partial/\partial\bar{\sigma}$ denote respectively the generalized derivatives

$$\frac{\partial}{\partial\sigma} = \frac{1}{2}\left(\frac{\partial}{\partial x} - \mathrm{i}\frac{\partial}{\partial y}\right) \quad \text{and} \quad \frac{\partial}{\partial\bar{\sigma}} = \frac{1}{2}\left(\frac{\partial}{\partial x} + \mathrm{i}\frac{\partial}{\partial y}\right), \tag{2.2}$$

where $\sigma = x + \mathrm{i}y$. The Beltrami equation

$$z_{\bar{\sigma}} = \lambda(\sigma) z_\sigma \tag{2.3}$$

is a special case of this equation. The function $\lambda(\sigma)$ in (2.3) is called complex dilation or Beltrami coefficient. Some discussion on the importance of the Beltrami equation (2.3) for the theory of quasiconformal mapping can be found in Ahlfors [2]. Ahlfors [1] and Vekua [29] define quasiconformal mapping of a domain Ω with complex dilation $\lambda(\sigma)$ as a homeomorphic generalized solution $z(\sigma)$ of the Beltrami equation. In order to preserve the orientation of quasiconformal mappings, this function is chosen to satisfy everywhere in the σ-plane the condition (see [15])

$$\left|\lambda(\sigma)\right| \leqslant \lambda_0 < 1. \tag{2.4}$$

The solution to the Beltrami equation (2.3) is usually written in terms of the following two integral operators:

$$T_1 f(\sigma) = -\frac{1}{\pi}\iint_{\Omega_R} \frac{f(\zeta)}{\zeta - \sigma}\,\mathrm{d}\xi\,\mathrm{d}\eta, \quad \sigma \in \Omega_R, \tag{2.5}$$

and

$$T_2 f(\sigma) = -\frac{1}{\pi}\iint_{\Omega_R} \frac{f(\zeta)}{(\zeta - \sigma)^2}\,\mathrm{d}\xi\,\mathrm{d}\eta, \quad \sigma \in \Omega_R, \tag{2.6}$$

where $\zeta = \xi + \mathrm{i}\eta$. The operator $T_2 f$ is to be understood as a Cauchy principal value and the function $f(\sigma)$ is assumed Hölder continuous. These two integral operators are known to satisfy the following relations (cf. [1]):

$$(T_1 f)_{\bar{\sigma}} = f(\sigma), \tag{2.7}$$

$$(T_1 f)_\sigma = T_2 f(\sigma). \tag{2.8}$$

Using the Cauchy–Green formula [4]

$$z(\sigma) = \frac{1}{2\pi}\int_{\partial\Omega_R} \frac{z(\zeta)}{\zeta - \sigma}\,\mathrm{d}\zeta - \frac{1}{\pi}\iint_{\Omega_R} \frac{z_{\bar{\zeta}}}{\zeta - \sigma}\,\mathrm{d}\xi\,\mathrm{d}\eta, \tag{2.9}$$

the solution of equation (2.3) (see Ahlfors [1] and Vekua [29]) can be written as

$$z(\sigma) = T_1 f(\sigma) + g(\sigma), \tag{2.10}$$

where

$$f(\sigma) = \lambda(\sigma) z_\sigma, \tag{2.11}$$

and $g(\sigma)$ is a suitable analytic function whose precise form depends on the boundary data. For example, for the problem of constructing the univalent solution of (2.3) as a mapping of the complex plane $\mathbb{C}$ onto itself, one puts $g(\sigma) = a\sigma + b$ or just $g(\sigma) = \sigma$ and takes $\Omega = \mathbb{C}$. It then follows from (2.8), (2.10) and (2.11) that

$$f(\sigma) = \lambda(\sigma)\bigl(T_2 f(\sigma) + g_\sigma(\sigma)\bigr), \tag{2.12}$$

which is a nonhomogeneous equation in the function $f(\sigma)$. The singular integral operator $T_2 f(\sigma)$ in (2.12) is a 2-dimensional Hilbert transform and is also known as a Beürling transform. It is an isometry of $L_2(\mathbb{C})$ onto $L_2(\mathbb{C})$ (cf. [9,24]), i.e.,

$$\bigl\|T_2 f(\sigma)\bigr\|_{L_2} = \|f\|_{L_2}, \tag{2.13}$$

which shows that equation (2.12) subject to the condition (2.4) has a unique square-integrable solution $f(\sigma)$. However, this does not rule out the unpleasant fact that the function $f \in L_2(\Omega)$ may be discontinuous. This causes difficulties for the theory of quasiconformal mappings where the continuity requirement is essential for any geometric interpretation. However, these problems do not arise and the solution (2.10) remains continuous if function $f(\sigma)$ is in Hölder space [24]. Therefore, the Beltrami equation (2.3) with $f(\sigma)$ in Hölder space has played a significant role in the study of quasiconformal mappings [24].

In the following section we describe a fast algorithm to solve a boundary value problem associated with a modified form of the homogeneous Beltrami equation (2.3) within an annulus. This will be the building block for the construction of quasiconformal mappings of doubly connected domains onto annuli described in section 4.

3. Dirichlet problem and its solution algorithm

We are interested in finding a function $w(\sigma)$ in an annulus Ω_R such that

$$\begin{cases} w_{\bar\sigma} = \lambda(\sigma) w_\sigma + \dfrac{\lambda(\sigma)}{\sigma} \equiv h(\sigma), & \sigma \in \Omega_R, \\ \mathrm{Real}\bigl(w\bigl(\sigma = \mathrm{e}^{\mathrm{i}\alpha}\bigr)\bigr) = u_1(\alpha), & 0 < \alpha \leqslant 2\pi, \\ \mathrm{Real}\bigl(w\bigl(\sigma = R\mathrm{e}^{\mathrm{i}\alpha}\bigr)\bigr) = u_R(\alpha), & 0 < \alpha \leqslant 2\pi, \\ \mathrm{Imag}\bigl[w(\sigma = 1)\bigr] = v_0, \end{cases} \tag{P}$$

where $\lambda(\sigma)/\sigma \to 0$ as $\sigma \to 0$ and $\lambda(\sigma)$ is Hölder continuous with $|\lambda(\sigma)| < 1$. It is known that this problem has a unique solution in the annulus Ω_R provided $u_R(\alpha)$ and $u_1(\alpha)$ satisfy appropriate compatibility condition. The partial differential equation in (P) is a nonhomogeneous Beltrami equation and is more convenient for our purposes as discussed later in section 4. This is obtained from homogeneous Beltrami equation (2.3) through the transformation $z(\sigma) = \sigma \mathrm{e}^{w(\sigma)}$ which we discuss in some detail in section 4.

Since the function $h(\sigma)$ in (P) depends on the solution $w(\sigma)$, an iterative algorithm has to be used to construct a solution of the problem (P) with the inhomogeneous term $h(\sigma)$ updated during each iteration level k based on the solution at previous iteration level $k-1$. However, at each iteration level the solution procedure is based on representation of $w(\sigma)$ as a T_1-transform of $h(\sigma)$ except for an additive analytic function $g(\sigma)$, similar to (2.10). It then follows that at each iteration level, the analytic function $g(\sigma)$ is to be updated as a solution of the following problem: find a $g(\sigma)$ in Ω_R such that

$$\begin{cases} g_{\bar\sigma} = 0, \quad \sigma \in \Omega_R, \\ \mathrm{Real}\big[g\big(\sigma = \mathrm{e}^{\mathrm{i}\alpha}\big)\big] = u_1(\alpha) - \mathrm{Real}\big(T_1 h\big(\sigma = \mathrm{e}^{\mathrm{i}\alpha}\big)\big), & 0 \leqslant \alpha \leqslant 2\pi, \\ \mathrm{Real}\big[g\big(\sigma = R\mathrm{e}^{\mathrm{i}\alpha}\big)\big] = u_R(\alpha) - \mathrm{Real}\big(T_1 h\big(\sigma = R\mathrm{e}^{\mathrm{i}\alpha}\big)\big), & 0 \leqslant \alpha \leqslant 2\pi, \\ \mathrm{Imag}\big[g(\sigma = 1)\big] = v_0 - \mathrm{Imag}\big(T_1 h(\sigma = 1)\big). \end{cases} \tag{RP}$$

This is a standard problem in the theory of complex variables and the solution to this problem can easily be constructed using Laurent series representation of the analytic function $g(\sigma)$ within the annulus. We denote the solution by

$$g(\sigma) = \Lambda\big(T_1 h(\alpha); u_R(\alpha), u_1(\alpha)\big), \tag{3.1}$$

where Λ denotes the solution operator of the above problem. Once this problem has been solved, solution of the problem (P) is constructed from

$$w(\sigma) = T_1 h(\sigma) + g(\sigma). \tag{3.2}$$

Algorithm 3.1. We see that equations (3.1), (3.2) and problem (P) suggest the following iteration scheme for solving the problem (P):

$$g^k(\sigma) = \Lambda\big(T_1 h^k(\alpha); u_R(\alpha), u_1(\alpha)\big), \tag{3.3}$$

$$h^{k+1}(\sigma) = \lambda(\sigma)\left[T_2 h^k(\sigma) + g^k_\sigma(\sigma) + \frac{1}{\sigma}\right]. \tag{3.4}$$

Here, the subscript k refers to the level of iteration. A suitable initial choice of $h(\sigma)$ starts the iteration procedure. Thereafter each kth level of iteration involves the following four steps:

(1) Find the $T_1 h^k(\alpha)$ on the boundary curves using the fast algorithm 3.2 described in [16].

(2) Construct the analytic function $g^k(\sigma)$ by solving the reduced problem (RP), as implicitly represented by (3.3).

(3) Find $T_2 h^k(\sigma)$ at all grid points in the annulus using the fast algorithm 3.2 described in [16].

(4) Compute $h^{k+1}(\sigma)$, updated value of $h(\sigma)$, using equation (3.4).

Once the converged function $h(\sigma)$ is found, the analytic function $g(\sigma)$ is computed from step 2 using this converged function $h(\sigma)$ and then $w(\sigma)$ is found using (3.2).

Remark 3.1. Notice that the above algorithm updates $h(\sigma)$ at the end of each iteration and this updated $h(\sigma)$ becomes the input for the next iteration. As discussed earlier, isometry of the operator T_2-transform implies that the operator $\tau h(\sigma)$ defined via

$$\tau h(\sigma) = \lambda(\sigma)\left\{T_2 h(\sigma) + \frac{1}{\sigma}\right\}$$

is a contraction in the space of Hölder continuous function. Therefore, there exists a unique h to which the scheme converges. The rate of convergence of the scheme depends on the initial guess of $h(\sigma)$. The fact that $h(\sigma) = \lambda(\sigma)w_\sigma + \lambda(\sigma)/\sigma$ suggests an initial guess of $h(\sigma) = 0$ provided $\lambda(\sigma) = \mathrm{O}(\varepsilon)$, $\varepsilon \ll 1$.

4. A numerical method for quasiconformal mapping

Let G be a doubly connected domain bounded by simple, closed and smooth curves Γ_0 and Γ_1 such that the point $z = 0$ lies inside the region bounded by Γ_0. The boundary curves Γ_0 and Γ_1 are given in parametric representation as follows:

$$\Gamma_0\colon\ \rho_0(\phi)\mathrm{e}^{\mathrm{i}\phi}, \quad 0 < \phi \leqslant 2\pi, \tag{4.1}$$

$$\Gamma_1\colon\ \rho_1(\phi)\mathrm{e}^{\mathrm{i}\phi}, \quad 0 < \phi \leqslant 2\pi. \tag{4.2}$$

We seek a quasiconformal mapping of a doubly connected domain G onto an annulus $\Omega_R = \{\sigma\colon\ R < |\sigma| < 1\}$ such that the inner boundary Γ_0 maps onto an as yet unknown inner circle of radius $R < 1$ and the outer boundary Γ_1 maps onto an outer circle of unit radius. In other words, we need to construct the solution of the following problem to find R and a map $z(\sigma)$, $\sigma \in \Omega_R$:

$$\begin{cases} z_{\bar\sigma} = \lambda(\sigma) z_\sigma, \quad \sigma \in \Omega_R, \\ z(\sigma)\colon \Gamma_1 \to \{\sigma\colon\ |\sigma| = 1\}, \\ z(\sigma)\colon \Gamma_0 \to \{\sigma\colon\ |\sigma| = R\}. \end{cases} \tag{QP}$$

The boundary curves Γ_0 and Γ_1 are assumed be convex. Therefore, their parameterizations $\phi_0(\alpha)$ and $\phi_1(\alpha)$ are monotonic functions of α, $0 \leqslant \alpha < 2\pi$. Since R is not known a priori, the complex dilation $\lambda(\sigma)$ which has Hölder continuous first derivative is specified a priori in the entire unit disk such that $|\lambda(\sigma)| < \lambda_0 < 1$ and $(\lambda(\sigma)/\sigma) \to 0$ as $\sigma \to 0$.

One of the possible ways to facilitate the determination of R is to induce the transformation

$$z(\sigma) = \sigma \mathrm{e}^{w(\sigma)} \tag{4.3}$$

in the homogeneous Beltrami equation defined in the boundary value problem (QP). A similar transformation has been used in Daripa [15], although for a different reason. The function $w(\sigma)$ defined through (4.3) satisfies the following nonhomogeneous Beltrami equation

$$w_{\bar\sigma} = \lambda(\sigma)w_\sigma + \frac{\lambda(\sigma)}{\sigma} \equiv h\big(w,\sigma,\bar\sigma\big), \qquad \sigma \in \Omega_R. \tag{4.4}$$

Below, we occasionally denote the function $h(w,\sigma,\bar\sigma)$ by $h(\sigma)$ for convenience. We have from (4.1)–(4.3),

$$\widetilde{w}_0(\alpha) = \ln\left(\frac{\tilde\rho_0(\alpha)}{R}\right) + \mathrm{i}\big(\phi_0(\alpha) - \alpha\big), \quad 0 \leqslant \alpha \leqslant 2\pi, \tag{4.5}$$

$$\widetilde{w}_1(\alpha) = \ln\tilde\rho_1(\alpha) + \mathrm{i}\big(\phi_1(\alpha) - \alpha\big), \qquad 0 \leqslant \alpha \leqslant 2\pi, \tag{4.6}$$

where we have used

$$\widetilde{w}_0(\alpha) = w\big(\sigma = R\mathrm{e}^{\mathrm{i}\alpha}\big), \quad \tilde\rho_0(\alpha) = \rho_0\big(\phi_0(\alpha)\big), \tag{4.7}$$

$$\widetilde{w}_1(\alpha) = w\big(\sigma = \mathrm{e}^{\mathrm{i}\alpha}\big), \quad \tilde\rho_1(\alpha) = \rho_1\big(\phi_1(\alpha)\big). \tag{4.8}$$

The boundary value problem (QP) is now equivalent to the following problem: find R and $w(\sigma)$, $R \leqslant |\sigma| \leqslant 1$, such that

$$\begin{cases} w_{\bar\sigma} = \lambda(\sigma)w_\sigma + \dfrac{\lambda(\sigma)}{\sigma} \equiv h(\sigma), & \sigma \in \Omega_R, \\ \mathrm{Real}\big(\widetilde{w}_1(\alpha)\big) = \ln\big(\tilde\rho_1(\alpha)\big) \equiv u_1(\alpha), & 0 < \alpha \leqslant 2\pi, \\ \mathrm{Real}\big(\widetilde{w}_0(\alpha)\big) = \ln\left(\dfrac{\tilde\rho_0(\alpha)}{R}\right) \equiv u_R(\alpha), & 0 < \alpha \leqslant 2\pi. \end{cases} \tag{RQP}$$

Even though $\tilde\rho_0(\alpha)$, $\tilde\rho_1(\alpha)$ and R are not known a priori, these can be updated during iterations required to solve this problem using the numerical method described in section 3. Since $\rho_0(\phi_0)$ and $\rho_1(\phi_1)$ are known from (4.1) and (4.2), $\tilde\rho_0(\alpha)$ and $\tilde\rho_1(\alpha)$ can be updated from the following equations which follow from (4.5) and (4.6):

$$\phi_0^k(\alpha) = \mathrm{Imag}\big(\widetilde{w}_0(\alpha)\big) + \alpha, \quad 0 < \alpha \leqslant 2\pi, \tag{4.9}$$

$$\phi_1^k(\alpha) = \mathrm{Imag}\big(\widetilde{w}_1(\alpha)\big) + \alpha, \quad 0 < \alpha \leqslant 2\pi. \tag{4.10}$$

Here, the superscripts k and $k+1$ refer to the level of iterations in the algorithm 3.1. To update R, we make use of the following relations which follow from the boundary conditions in (RQP).

$$F(R) = \int_0^{2\pi} \big(R\mathrm{e}^{u_R(\alpha)} - \tilde\rho_0(\alpha)\big)\,\mathrm{d}\alpha = 0, \tag{4.11}$$

$$F(0) = -\int_0^{2\pi} \tilde\rho_0(\alpha)\,\mathrm{d}\alpha < 0, \tag{4.12}$$

$$F(1) = \int_0^{2\pi} \left(\mathrm{e}^{u_1(\alpha)} - \tilde{\rho}_0(\alpha)\right) \mathrm{d}\alpha$$
$$= \int_0^{2\pi} \left(\rho_1\left(\phi_1(\alpha)\right) - \rho_0\left(\phi_0(\alpha)\right)\right) \mathrm{d}\alpha \; > 0. \qquad (4.13)$$

Note that the second inequality in (4.13) does not strictly follow unless $\mathrm{d}\alpha$ is replaced with $\mathrm{d}\phi$. However, since there is only one value of R for which (4.11) must hold, (4.13) has to be true in light of (4.12). Due to inequalities (4.12) and (4.13), a bisection method can be applied to equation (4.11) to find R.

A formal description of the algorithm for the quasiconformal mapping method that has been successful in our numerical experiments is given below. The quasiconformal mapping method involves two levels of iterations. It solves a sequence of problems (RQP), each with different R and boundary values, in an iterative loop which constitutes what we call "outer" iteration for later reference. Each problem (RQP) for a fixed choice of R and given boundary values is solved by solving a sequence of problems (P) defined in section 3, each with a different function $h(\sigma)$, in an iterative loop which constitutes what we call "inner" iteration for later reference. The solution method for solving (P) is discussed in section 3.

Algorithm 4.1.

Comment [Initialize $\phi_0(\alpha)$ and $\phi_1(\alpha)$. Also set values to r_1 and r_2]
Choose $\phi_0^0(\alpha) = \phi_1^0(\alpha) = \alpha$. Set $r_1 = 0$ and $r_2 = 1.0$.

Comment [Solve for R and $z(\sigma)$]
do $k = 0, \ldots, n$

Step 1.
Set $R^k = 0.5(r_1 + r_2)$, $\tilde{\rho}_0^k = \rho_0(\phi_0^k(\alpha))$ and $\tilde{\rho}_1^k = \rho_1(\phi_1^k(\alpha))$.

Step 2.
Solve problem (RQP) to compute $w^{k+1}(\sigma)$, $\phi_0^{k+1}(\alpha)$ and $\phi_1^{k+1}(\alpha)$ within the annulus using the numerical method described in section 3.

Step 3.
Compute the value of the integral $F(R^k)$ using equation (4.11).

Step 4.
Comment [Reset values of r_1 and r_2]
If $F(R^k) < 0$, then set $r_1 = R^k$ and go to step 5. If $F(R^k) > 0$, then set $r_2 = R^k$ and go to step 5. If $R = R^k$, then go to step 6.

Step 5.
If $|r_2 - r_1| \leqslant \varepsilon$, then go to step 5. If $|r_2 - r_1| > \varepsilon$, then go to step 1.

Step 6.
Comment [Find $z(\sigma)$ using (4.3)]
$z = \sigma \mathrm{e}^{w(\sigma)}$.
Stop
end do

5. Numerical results

We have carried out some numerical experiments with the quasiconformal mapping method presented in the previous section. Most numerical results to be presented below pertain to the following complex dilation (cf. [15]):

$$\lambda_1(\sigma) = |\sigma|^2 \mathrm{e}^{0.65(\mathrm{i}\sigma^5 - 2.0)}. \tag{5.1}$$

We should mention that similar numerical experiments with another complex dilation (cf. [15]), namely

$$\lambda_2(\sigma) = 0.5|\sigma|^2 \sin\bigl(2.5(\sigma + \bar{\sigma})\bigr), \tag{5.2}$$

have been equally successful and the numerical results are not terribly different or interesting from the viewpoint of what has already been presented below for the case of complex dilation $\lambda_1(\sigma)$. Therefore, few results will be presented with $\lambda = \lambda_2$. It is worth emphasizing that dilations $\lambda_1(\sigma)$ and $\lambda_2(\sigma)$ have been used previously by Daripa [15] for quasiconformal mapping of exterior of simply connected domains onto the interior of a unit disk. There is no physical motivation behind selection of these choices of dilation. Some discussions on these choices of dilation can be found in Daripa [15].

We present results for the following six doubly connected domains defined by their boundary curves Γ_0 and Γ_1, each defined parametrically as a periodic function of the parameter ϕ for $0 \leqslant \phi < 2\pi$. The inner and outer boundaries of each of the following domains are similar for domains 2–4. For the rest three domains, inner and outer boundaries are dissimilar.

(1) Domain 1: $\Gamma_0 := 0.5\mathrm{e}^{\mathrm{i}\phi}$, $\Gamma_1 := (1 + 0.08 \sin 4\phi)\,\mathrm{e}^{\mathrm{i}\phi}$.

(2) Domain 2: $\Gamma_0 := \bigl(\cos^8\phi + \sin^8\phi\bigr)^{-1/8}\mathrm{e}^{\mathrm{i}\phi}$, $\Gamma_1 := 2\bigl(\cos^8\phi + \sin^8\phi\bigr)^{-1/8}\mathrm{e}^{\mathrm{i}\phi}$.

(3) Domain 3: $\Gamma_0 := 0.3\sqrt{1 - 0.75\cos^2\phi}\,\mathrm{e}^{\mathrm{i}\phi}$, $\Gamma_1 := \sqrt{1 - 0.75\cos^2\phi}\,\mathrm{e}^{\mathrm{i}\phi}$.

(4) Domain 4: $\Gamma_0 := (0.7 + 0.056 \sin 4\phi)\,\mathrm{e}^{\mathrm{i}\phi}$, $\Gamma_1 := (1 + 0.08 \sin 4\phi)\,\mathrm{e}^{\mathrm{i}\phi}$.

(5) Domain 5: $\Gamma_0 := 0.2\bigl(\cos^8\phi + \sin^8\phi\bigr)^{-1/8}\mathrm{e}^{\mathrm{i}\phi}$, $\Gamma_1 := (1 + 0.08 \sin 4\phi)\,\mathrm{e}^{\mathrm{i}\phi}$.

(6) Domain 6: $\Gamma_0 := 0.3324\mathrm{e}^{\mathrm{i}\phi}$, $\Gamma_1 := (1 + 0.09 \sin 8\phi)\,\mathrm{e}^{\mathrm{i}\phi}$.

For each of the above domains, calculations were carried out in 7-digit arithmetics with $N = 64, 128, 256$ for each of $M = 13, 26, 51$. The numerical method converged with respect to iterations for each of these choices of number of grid points and complex dilation. The method also appears to converge with respect to grid refinement and a result of a typical case in this regard is presented later. The mappings for the above six domains, namely, domains 1–6 are presented in figure 1 when $N = 256$, $M = 51$ and tolerance $\varepsilon = 0.00004$. The plots in this figure show the images of some of the circular and radial grid lines onto the doubly connected domains with $\lambda = \lambda_1$. In each of these cases, R is determined numerically as part of the numerical procedure. In

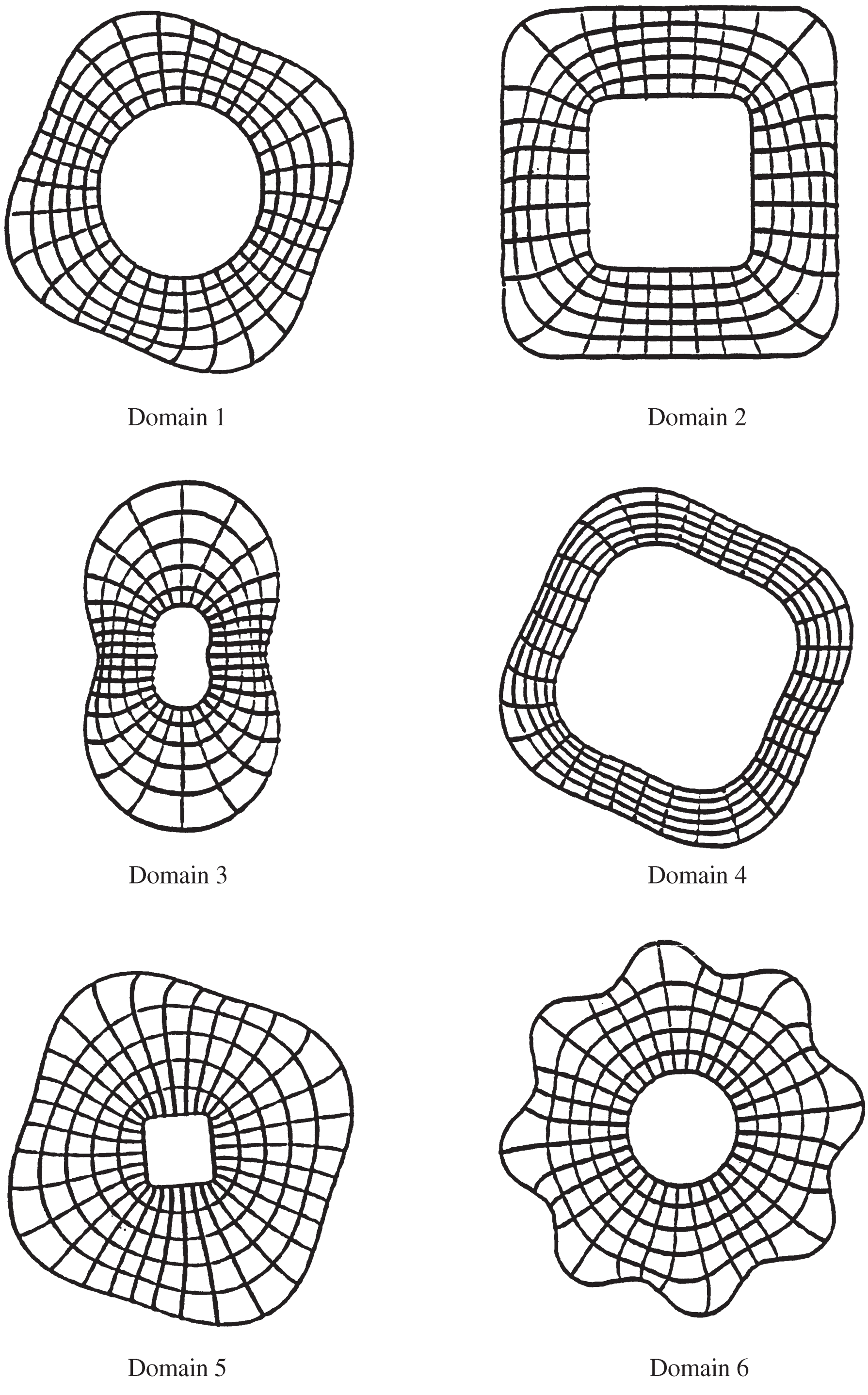

Figure 1. Quasiconformal mapping of the domains 1–6 with $\lambda = \lambda_1$ given by (5.1).

Table 1
Summary of numerical results for the twelve case studies.

Example	Converged value of R	Number of inner iterations	Number of outer iterations
Domain-1, $\lambda = \lambda_1$	0.506989	10	14
Domain-1, $\lambda = \lambda_2$	0.504608	9	15
Domain-2, $\lambda = \lambda_1$	0.527130	14	12
Domain-2, $\lambda = \lambda_2$	0.520966	16	15
Domain-3, $\lambda = \lambda_1$	0.329193	26	15
Domain-3, $\lambda = \lambda_2$	0.356781	26	15
Domain-4, $\lambda = \lambda_1$	0.709198	10	13
Domain-4, $\lambda = \lambda_2$	0.703644	11	15
Domain-5, $\lambda = \lambda_1$	0.232330	13	15
Domain-5, $\lambda = \lambda_2$	0.233734	15	15
Domain-6, $\lambda = \lambda_1$	0.342926	15	15
Domain-6, $\lambda = \lambda_2$	0.343170	17	15

table 1, converged values of R, number of inner iterations for converged values of R and number of outer iterations are presented for each of these doubly connected domains for both choices of dilation. It also shows the convergence results for the case $\lambda = \lambda_2$.

In figure 2, various convergence results are presented for the case of domain 1. The number of outer iterations in this case is 14 and the number of inner iterations with the converged value of R is 10. In figure 2(a) we show the convergence of $F(R)$ to zero within few iterations (see equation (4.11)). Figure 2(b) shows convergence of R to a value 0.506989 within a modest number of iterations. Convergence rate of R during outer iterations is shown in figure 2(c). In figure 2(d) we have plotted L_∞ error in w when $R = 0.506989$ against the level of iterations. In figure 2(e), convergence rate of L_∞ error in w when $R = 0.506989$ is shown. These results show the rapid convergence properties of the quasiconformal mapping method.

Figure 3 depicts numerical results for domain 3. A comparison of this figure with figure 2 shows that qualitative behaviors of $F(R)$ and R against number of iterations for domain 3 are different from those for domain 1. Qualitative behaviors of all other convergence results for domain 3 are almost similar to those for domain 1.

Figures 2 and 3 are representatives of numerical results for all other domains listed previously and for both choices of dilation. Instead of showing such similar results, we summarize the following pertinent observations, some of which may not be clear from the figures or tables presented here.

- The qualitative behaviors of the convergence of $F(R)$ and R with respect to iterations are similar for each of the domains. However, these may be different for different domains.
- The number of inner iterations with the converged value of R is less than 10 for each of these domains.

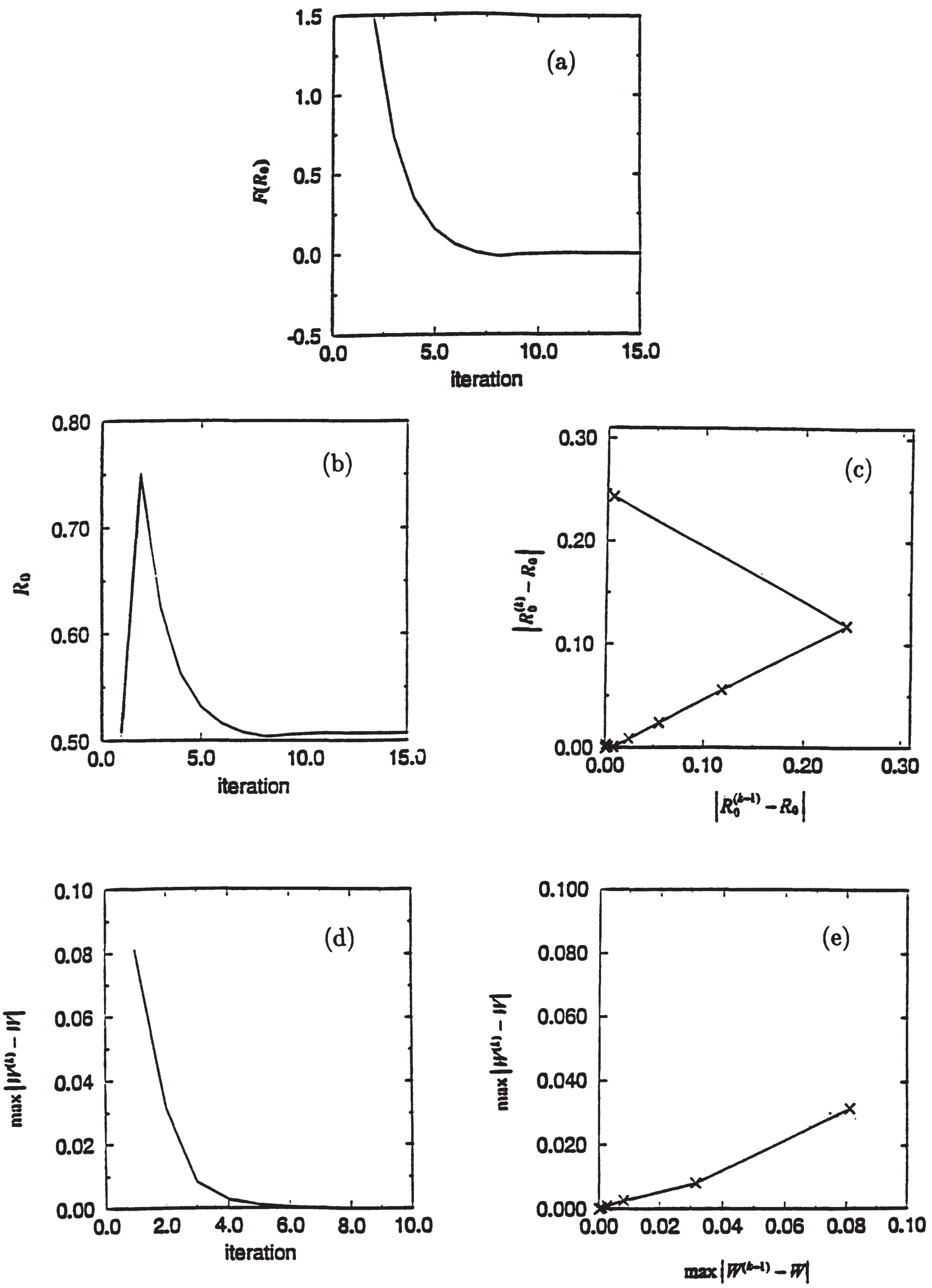

Figure 2. Convergence results for quasiconformal mapping of domain 1 with $\lambda = \lambda_1$ given by (5.1): (a) convergence of $F(R)$ given by (4.11); (b) convergence of R; (c) convergence *rate* of R; (d) convergence of w when $R = 0.506989$; (e) convergence *rate* of w when $R = 0.506989$.

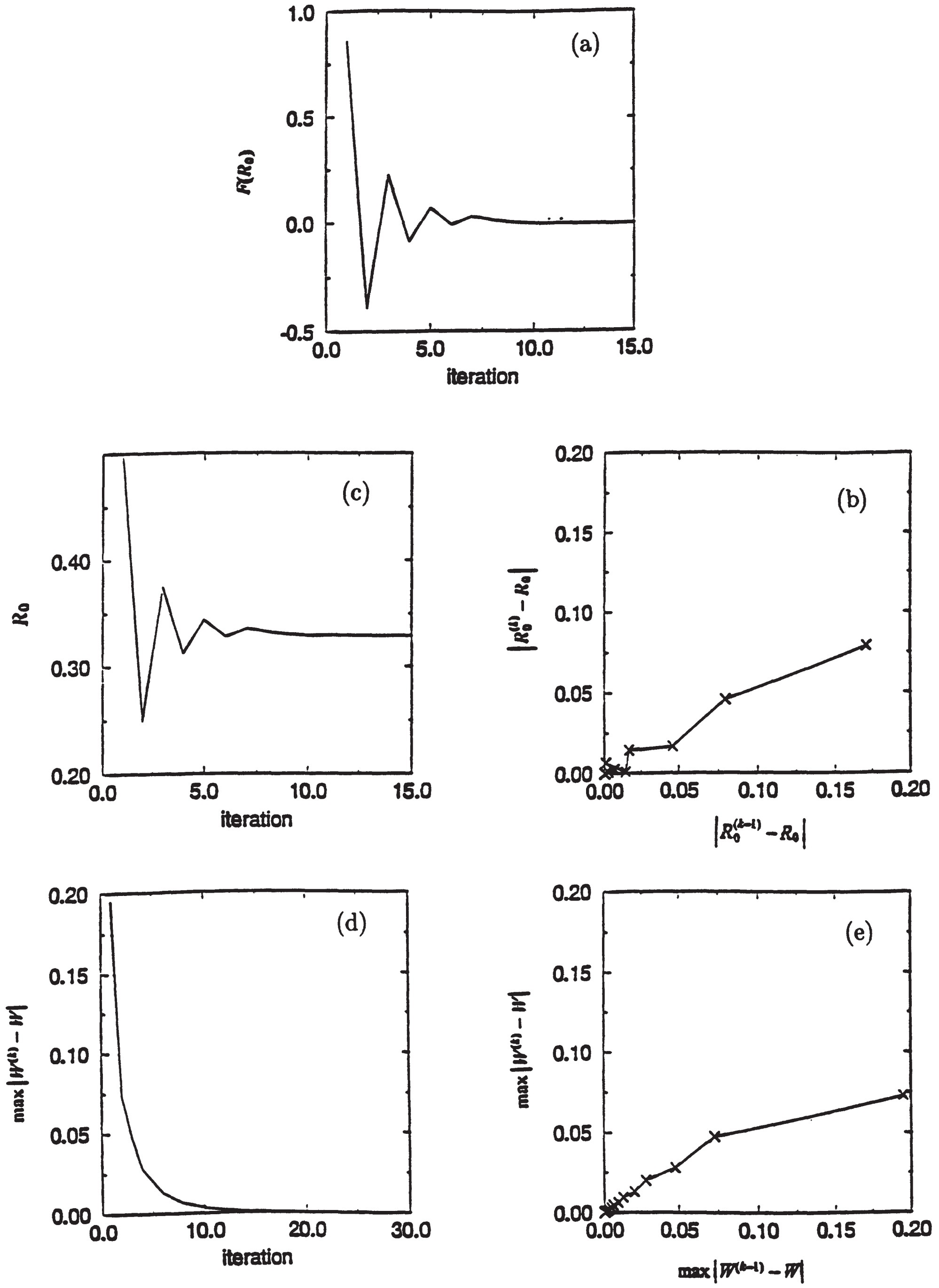

Figure 3. Convergence results for quasiconformal mapping of domain 3 with $\lambda = \lambda_1$ given by (5.1): (a) convergence of $F(R)$ given by (4.11); (b) convergence of R; (c) convergence *rate* of R; (d) convergence of w when $R = 0.329193$; (e) convergence *rate* of w when $R = 0.329193$.

Table 2
Convergence of R with respect to M for domain 6 when $N = 256$, $\lambda = \lambda_2$.

M	R	Error in R	Number of inner iterations	Number of outer iterations
51	0.343170	0	17	15
26	0.342743	4.27×10^{-4}	16	15
13	0.342743	4.27×10^{-4}	16	15

Table 3
Convergence of R with respect to N for domain 6 when $M = 51$, $\lambda = \lambda_2$.

N	R	Error in R	Number of inner iterations	Number of outer iterations
256	0.343170	0	17	15
128	0.333099	0.010071	10	15
64	0.329620	0.01355	9	15

- The number of outer iterations is about the same for each of these domains.
- The rate of convergence of R is linear.

Since we have not shown any example with $\lambda = \lambda_2$, we feel it may be worthwhile to present few results with this choice of the dilation. Figure 4 shows the quasiconformal mappings of domain 5 and domain 6 with $\lambda = \lambda_2$. In tables 2 and 3, we show the values of R for the domain 6 when $\lambda = \lambda_2$ for various choices of N and M. The L_∞ error in R in these tables has been measured with respect to the results obtained with $N = 256$ and $M = 51$. The numbers of inner as well as outer iterations are shown in these tables. From these tables and from similar experiments, we made the following observations:

- Convergence of R is slow with respect to N but is faster with respect to M.
- Number of outer iterations depends very mildly on the number of grid points. In the cases shown in tables 2 and 3, it does not depend on the number of grid points.
- Number of inner iterations depends on the number of grid points, weakly on M but somewhat strongly on N.

6. Summary and conclusion

We have presented and implemented an efficient numerical method for quasiconformal mappings of doubly connected domains onto annuli with a given complex dilation $|\lambda(\sigma)| \leqslant \lambda_0 < 1$. The ratio R of the radii of the annulus within which the nonlinear equation is to be solved is unknown a priori. An iterative procedure is used to update the R. During each such iteration, a nonhomogeneous Beltrami equation is solved using an iterative method within a known annulus. Thus, there are two levels of iterations: the inner iteration that updates the solution of an appropriate boundary

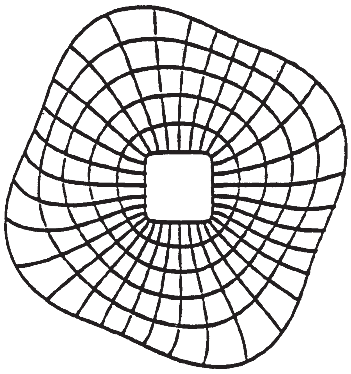

Domain 5

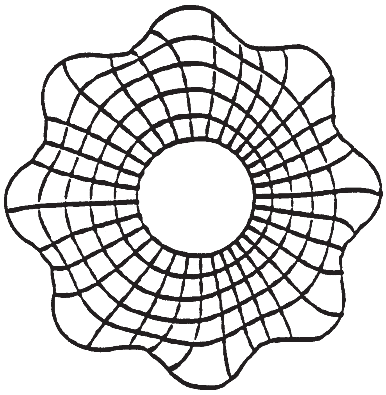

Domain 6

Figure 4. Quasiconformal mapping of the domains 5–6 with $\lambda = \lambda_2$ given by (5.2).

value problem within a known annulus and the outer iteration that updates R. We have argued using a fixed point theorem that the inner iteration converges. We have also given numerical evidence of this through numerical examples. The whole iterative procedure of determining the annulus as well as the solution inside this annulus is what constitutes the quasiconformal method. We have given no proof of convergence of the outer iterations, or equivalently of the quasiconformal mapping method. However, from numerical experiments it appears that the quasiconformal mapping method converges, at least for the set of examples presented here.

This method is computationally very efficient because the number of iterations are few and, more importantly, it uses the fast algorithm of Daripa [14,16]) for evaluating the singular operators that arise in this quasiconformal mapping method.

Finally, we want to mention the following areas of current (some ongoing) and future research:

- Numerical experiments with more complicated domains and with realistic dilation should be carried out.
- Construction of quasiconformal mapping methods with dilation specified in the doubly connected domain is an area of future work.
- In many practical problems [5,12–16], the Beltrami equation itself is required to be solved in arbitrary domains whose boundaries may not be circular. Development of similar efficient and spectrally accurate algorithms for solving the Beltrami equation in an arbitrary domain is nontrivial because the fast algorithms for the singular integral operators [14,16] which are used here do not easily extend to more general domains. This is an area of future work.
- A conformal mapping method based on the transformation (4.3) can be constructed and may be competitive with other conformal mapping methods of doubly connected domains onto annuli. This is also an area of future work.
- Extension of our method for domains with corners is another area of future work.
- A theoretical proof of convergence of the quasiconformal mapping method is an area of future work.
- Lastly, practical applications of quasiconformal mapping methods need to be further explored. Some are mentioned in section 1.

Acknowledgements

This material is based in part upon work supported by the Texas Advanced Research Program under Grant No. TARP-97010366-030. This research is also partly supported by the NSF under Grants No. DMS-9208061 and by the Office of the Vice President for Research and Graduate Studies at Texas A&M University. The allocation of computer resources by the Texas A&M Supercomputer Center is gratefully acknowledged. The authors also acknowledge the suggestions made by the referees.

References

[1] L.V. Ahlfors, Conformality with respect to Riemannian matrices, Ann. Acad. Sci. Fenn. Ser. AI 206 (1955) 1–22.

[2] L.V. Ahlfors, *Lectures in Quasiconformal Mappings* (Van Nostrand Reinhold, New York, 1966).

[3] P.P. Belinskii, S.K. Godunov and I.K. Yanenko, The use of a class of quasiconformal mappings to construct difference nets in domains with curvilinear boundaries, USSR Comp. Math. Phys. 15 (1975) 133–144.

[4] S.R. Bell, *The Cauchy Transform, Potential Theory and Conformal Mapping* (CRC Press, New York, 1992).

[5] L. Bers, *Mathematical Aspects of Subcritical and Transonic Gas Dynamics* (Wiley, New York, 1958).

[6] L. Bers, Quasiconformal mappings, with applications to differential equations, function theory and topology, Amer. Math. Soc. Bull. 83(6) (1977) 1083–1100.

[7] L. Bers and L. Nirenberg, On a representation theorem for linear elliptic systems with discontinuous coefficients and its applications, in: *Convegno Internazionale Suelle Equaziono Cremeonese*, Roma (1955) pp. 111–140.

[8] L. Bers and L. Nirenberg, On linear and nonlinear elliptic boundary value problems in the plane, in: *Convegno Internazionale Suelle Equaziono Cremeonese*, Roma (1955) pp. 141–167.

[9] B. Bojarski and T. Iwaniec, Quasiconformal mappings and nonlinear elliptic equations in two variables I, II, Bull. Acad. Polon. Sci. Sér. Math. Astronom. Phys. 12 (1974) 473–478 and 479–484.

[10] L. Carleson and T. Gamelin, *Complex Dynamics* (Springer, New York 1993).

[11] R. Courant and D. Hilbert, *Methods of Mathematical Physics*, Vol. II (Wiley, New York, 1961).

[12] P. Daripa, On applications of a complex variable method in compressible flows, J. Comput. Phys. 88 (1990) 337–361.

[13] P. Daripa, On a numerical method for quasiconformal grid generation, J. Comput. Phys. 96 (1991) 229–236.

[14] P. Daripa, A fast algorithm to solve nonhomogeneous Cauchy–Riemann equations in the complex plane, SIAM J. Sci. Statist. Comput. 13(6) (1992) 1418–1432.

[15] P. Daripa, A fast algorithm to solve the Beltrami equation with applications to quasiconformal mappings, J. Comput. Phys. 106(2) (1993) 355–365.

[16] P. Daripa and D. Mashat, Singular integral transforms and fast numerical algorithms, Numer. Algorithms, this issue.

[17] G.M. Goluzin, *Geometric Theory of Function of a Complex Variable* (Wiley, New York, 1969).

[18] H. Grötzsch, Über die Verzerrung bei schlichten nichtkonformen Abbildungen und eine damit zusammenhängende Erweiterung des Picardschen, Rec. Math. 80 (1928) 503–507.

[19] M.A. Lavrentjev, Sur une classe de représentations continues, Rec. Math. 48 (1935) 407–423.

[20] O. Lehto and K.I. Virtanen, *Quasiconformal Mapping in the Plane*, 2nd ed. (Springer, Berlin, 1973).

[21] C.W. Mastin and J.F. Thompson, Discrete quasiconformal mappings, Z. Angew. Math. Phys. 29 (1978) 1–11.

[22] C.W. Mastin and J.F. Thompson, Quasiconformal mappings and grid generation, SIAM J. Sci. Statist. Comput. 5(2) (1984) 305–310.

[23] C.B. Morrey, On the solutions of quasi-linear elliptic differential equations, Trans. Amer. Math. Soc. 43 (1938) 126–166.

[24] A. Mshimba and W. Tutschke, *Functional Analytic Methods in Complex Analysis and Applications to Partial Differential Equations* (World Scientific, Singapore, 1990).

[25] L. Nirenberg, On nonlinear elliptic differential equations and Hölder continuity, Comm. Pure Appl. Math. 6 (1953) 103–156.

[26] L. Nirenberg, On a generalization of quasiconformal mappings and its applications to elliptic partial differential equations, in: *Contributions to the Theory of Partial Differential Equations*, eds. L. Bers et al., Annals of Mathematics Studies 33 (Princeton Univ. Press, Princeton, NJ, 1954) pp. 95–100.

[27] W.H. Press, *Numerical Recipes in Fortran*, 2nd ed. (Cambridge Univ. Press, Cambridge, 1992).

[28] Z.V. Samsoniya, Quasiconformal mapping of multiply connected domains, Proc. of the Institute of Computational Mathematics, Georgian Academy of Sciences 25 (1985) 120–135 (in Russian).

[29] I.V. Vekua, The problem of reducing differential forms of elliptic type to canonical form and the generalized Cauchy–Riemann system, Doklady Akad. Nauk USSR 100 (1955) 197–200 (in Russian).

[30] A.P. Vlasyuk, Automatic construction of conformal and quasiconformal mapping of doubly connected and triple connected domains, Akad. Nauk Ukrainy Inst. Mat., preprint (Akademiya Nauk Ukrainy Institut Matematiki, preprint) 57 (1991) 1–57.

[31] J. Weisel, Numerische Ermittlung quasikonformer Abbildungen mit finiten Elementen, Numer. Math. 35 (1980) 201–222.